| Faculty and Researchers | Faculty and Researchers' Publications |

On the pressure gradient force over steep topography in sigma coordinate ocean models

Haney, Robert L.

American Meteorological Society

NOTES AND CORRESPONDENCE

On the Pressure Gradient Force over Steep Topography in Sigma Coordinate Ocean Models

ROBERT L. HANEY

Department of Meteorology, Naval Postgraduate School, Monterey, California

12 January 1990 and 15 October 1990

ABSTRACT

The error in computing the pressure gradient force near steep topography using terrain following (σ) coordinates is investigated in an ocean model using the family of vertical differencing schemes proposed by Arakawa and Suarez. The truncation error is estimated by substituting known buoyancy profiles into the finite difference hydrostatic and pressure gradient terms. The error due to "hydrostatic inconsistency," which is not simply a space truncation error, is also documented. The results show that the pressure gradient error is spread throughout the water column, and it is sensitive to the vertical resolution and to the placement of the grid points relative to the vertical structure of the buoyancy field being modeled. Removing a reference state, as suggested for the atmosphere by Gary, reduces the truncation error associated with the two lowest vertical modes by a factor of 2 to 3. As an example, the error in computing the pressure gradient using a standard 10-level primitive equation model applied to buoyancy profiles and topographic slopes typical of the California Current region corresponds to a false geostrophic current of the order of 10–12 cm s^{-1}. The analogous error in a hydrostatically consistent 30-level model with the reference state removed is about an order of magnitude smaller.

1. Introduction

In terrain following (σ) coordinates, the pressure gradient force is the sum of two terms. One term involves the gradient of pressure along a constant σ-surface and the other involves the gradient of bottom topography. Near steep topography these terms are large, comparable in magnitude, and opposite in sign. In such a case, a small error in computing either term near steep topography can result in a large error in the total pressure gradient force. Since large topographic slopes are common in the ocean, it is important to know the accuracy with which oceanic flows over abrupt topography can be modeled using the primitive equations in σ-coordinates. The purpose of this study is to investigate a number of schemes for the pressure gradient force in the context of an ocean model and to document the ability of the schemes to compute an accurate pressure gradient force over steep topography.

Meteorologists working in numerical weather prediction have been aware of the difficulties of modeling flow over steep topography for a long time. In particular, a number of methods have been proposed to reduce the error in the pressure gradient force when using σ-coordinates. For example, Corby et al. (1972) and Simmons and Burridge (1981) developed a vertical finite difference scheme for the hydrostatic equation in

which the pressure gradient is exact when the temperature is a linear function of the natural logarithm of pressure. Following Corby et al. (1972) and Simmons and Burridge (1981), Arakawa and Suarez (1983) derived a family of numerical schemes for the primitive equations of atmospheric motion in σ-coordinates in which the pressure gradient is exact for certain atmospheres. The schemes also retain other important properties of the continuous equations. Arakawa and Suarez (1983) expected that with no error in the pressure gradient for this given, typical, atmosphere, large errors would be avoided in more general cases.

Using a different approach, Gary (1973) showed that the size of the two terms in the pressure gradient in σ-coordinates is reduced, and the truncation error therefore reduced, if a horizontally uniform reference state density field, and its associated hydrostatic pressure field, is removed before computing the individual pressure gradient terms. Gary's results were confirmed by Johnson and Uccellini (1983) who found that the pressure gradient error in the case of stratified flow over an isolated mountain was reduced by a factor of four when an adiabatic reference state was removed from the hydrostatic equation. However, Sundqvist (1975, 1976) distinguished between truncation errors due to horizontal differencing and vertical differencing, and showed that the most significant errors are produced by sharp temperature inversions such as those that occur at the tropopause. Sundqvist also noted that the pressure gradient error is not likely to be reduced

by subtracting a reference state because it is the higher vertical modes that cause the most difficulties in the difference formulations. In the case of the atmosphere therefore, it is not entirely clear how much the pressure gradient error can be reduced, in general, by simply removing a reference state. In the case of the ocean, the technique might prove useful in limited area models where the departure of the density from a suitably chosen reference state is relatively small. However, it may be of little help in global models where the density difference from a given reference state is not small. The effect of removing a reference state in the ocean is documented below.

In addition to the truncation error problem, Rousseau and Pham (1971), Janjić (1977), and Mesinger (1982) have identified a problem of "hydrostatic consistency" associated with the σ-coordinate system. A sufficient condition for a finite difference scheme to be hydrostatically consistent is, in terms of the notation used below,

$$\left| \frac{\sigma}{D} \frac{\partial D}{\partial x} \right| \delta x < \delta \sigma. \qquad (1)$$

This condition, which requires a sufficiently small grid size for a given vertical grid increment, guarantees that the σ-surface immediately below (above) a given σ-surface remains below (above) the given σ-surface within a horizontal distance of one grid interval. If (1) is not satisfied, the finite difference scheme is hydrostatically inconsistent and nonconvergent (Mesinger and Janjić, 1985). The importance of this requirement is emphasized below.

Using the above meterological experience and research as background, this study analyzes and documents the errors in computing the pressure gradient force in σ-coordinate ocean models. This is done by computing the truncation error for known analytic profiles of density and pressure that are typical of the real ocean. The results show the level of accuracy that is attainable, and the horizontal and vertical resolution that is required, to compute the pressure gradient force near steep topography in σ-coordinate ocean models.

2. The horizontal pressure gradient in σ-coordinates

The horizontal pressure gradient in the x-direction is written in σ-coordinates as

$$\left. \frac{\partial p}{\partial x} \right)_z = \left. \frac{\partial p}{\partial x} \right)_\sigma - \frac{\sigma}{D} \frac{\partial p}{\partial \sigma} \frac{\partial D}{\partial x}, \qquad (2)$$

where p is pressure, z is height measured upward from the undisturbed sea surface, D the ocean depth, and $\sigma = z/D < 0$ the nondimensional, terrain-following vertical coordinate. The hydrostatic equation in σ-coordinates is

$$\frac{\partial p}{\partial \sigma} = -\rho g D \qquad (3)$$

where ρ is density and g is gravity. As indicated in the Introduction, we want to examine the effect on the pressure gradient of removing a reference state that depends only on z from each of the terms in (2). Toward this end, ρ is expressed in terms of a reference state that depends only on z, $\bar{\rho}(z)$, and a deviation from that state, ρ'

$$\rho = \bar{\rho} + \rho'. \qquad (4)$$

Substituting (4) into (3) and integrating allows the pressure to be expressed as

$$p = p_0 + \bar{p} + p',$$

where $p_0 = p(x, y, 0, t)$ is the pressure at $\sigma = 0$, and

$$\bar{p} = \int_\sigma^0 \bar{\rho} g D d\varsigma \qquad (5)$$

$$p' = \int_\sigma^0 \rho' g D d\varsigma. \qquad (6)$$

In a *rigid lid* model, the external mode and the internal modes are computed separately. The pressure gradient force that drives the internal modes in such a model is the difference between the pressure gradient and the vertical average of the pressure gradient. This internal pressure gradient force is independent of p_0. Since $\bar{p}$ is a function of z only, the hydrostatic equation in z coordinates can be used to show that $\bar{p}$ is also a function of z only. Thus, from (4), the internal pressure gradient force is

$$\left. \widehat{\frac{\partial p}{\partial x}} \right)_z \equiv \left. \frac{\partial p}{\partial x} \right)_z - \frac{1}{D} \int_{-D}^0 \left. \frac{\partial p}{\partial x} \right)_z dz$$

$$= \left. \frac{\partial p'}{\partial x} \right)_z - \frac{1}{D} \int_{-D}^0 \left. \frac{\partial p'}{\partial x} \right)_z dz. \qquad (7)$$

Using (2), the last two terms can be expressed in σ-coordinates as

$$\left. \widehat{\frac{\partial p}{\partial x}} \right)_z = \frac{\partial p'}{\partial x} - \frac{\sigma}{D} \frac{\partial p'}{\partial \sigma} \frac{\partial D}{\partial x}$$

$$- \int_{-1}^0 \left[\frac{\partial p'}{\partial x} - \frac{\sigma}{D} \frac{\partial p'}{\partial \sigma} \frac{\partial D}{\partial x} \right] d\sigma. \qquad (8)$$

Since only the disturbance part of the pressure appears on the right-hand side of (8), the individual terms are much smaller, and the truncation errors are perhaps smaller, than they would be if the reference state were not removed (Gary 1973). This point is addressed below (Tables 1 and 2).

In using (8) to compute the internal pressure gradient force it is convenient to introduce the disturbance buoyancy b,

$$b = -\frac{\rho'}{\rho_0} g, \qquad (9)$$

TABLE 1. Pressure gradient error (cm s^{-1}). Reference state removed.

Mode number	Vertical resolution (K)						
	5	10	15	20	25	30	35
1	3.99	0.95	0.40	0.22	0.16	0.09	0.07
2	3.63	1.72	0.81	0.45	0.29	0.20	0.14
3	18.90	3.43	1.57	0.97	0.57	0.42	0.30

where ρ_0 is a constant reference density. Defining B by

$$B = \int_\sigma^0 b \, d\zeta \qquad (10)$$

$$\frac{\partial B}{\partial \sigma} = -b, \qquad (11)$$

allows the disturbance hydrostatic equation (6) to be written as

$$p' = -\rho_0 DB, \qquad (12)$$

$$\frac{\partial p'}{\partial \sigma} = \rho_0 Db. \qquad (13)$$

Using (12) and (13), the internal pressure gradient force can be written in terms of b and B as

$$\frac{1}{\rho_0} \left. \frac{\widehat{\partial p}}{\partial x} \right)_z = -\left(\frac{\partial}{\partial x}(DB) + \sigma b \frac{\partial D}{\partial x} \right)$$

$$+ \int_{-1}^0 \left(\frac{\partial}{\partial x}(DB) + \sigma b \frac{\partial D}{\partial x} \right) d\sigma. \qquad (14)$$

The finite difference schemes for the internal pressure gradient are based on (10), (11) and (14). Three special cases are of interest.

If b is constant in the vertical, $b = b(x, y, t)$, then $B = -\sigma b$ from (10) and

$$\int_{-1}^0 \sigma b \, d\sigma = -\frac{1}{2} b. \qquad (15)$$

Using these in (14) yields

$$\frac{1}{\rho_0} \left. \frac{\widehat{\partial p}}{\partial x} \right)_z = \left(\sigma + \frac{1}{2} \right) D \frac{\partial b}{\partial x}. \qquad (16)$$

If b varies only in the vertical, $b = b(z)$, then

$$\frac{\partial b}{\partial x} = \frac{\sigma}{D} \frac{\partial b}{\partial \sigma} \frac{\partial D}{\partial x}. \qquad (17)$$

Using this along with (10), the first two terms on the right side of (14) become

$$\frac{\partial}{\partial x}(DB) + \sigma b \frac{\partial D}{\partial x} = D \int_\sigma^0 \frac{\partial b}{\partial x} d\zeta$$

$$+ \left(\int_\sigma^0 b \, d\zeta + \sigma b \right) \frac{\partial D}{\partial x}$$

$$= \left(\int_\sigma^0 \frac{\partial}{\partial \zeta}(\zeta b) d\zeta + \sigma b \right) \frac{\partial D}{\partial x}$$

$$= 0. \qquad (18)$$

Thus, a density field that varies only in the vertical (such as a z-dependent reference state) produces no horizontal pressure gradient.

If the disturbance buoyancy varies along the isobaths as well as in the vertical, say $b = b(y, z)$, then the same procedure that led to (18) now gives

$$\frac{\partial}{\partial x}(DB) + \sigma b \frac{\partial D}{\partial x} = D \int_\sigma^0 \frac{\sigma'}{D} \frac{\partial b}{\partial \sigma'} \frac{\partial D}{\partial x} d\sigma'$$

$$+ B \frac{\partial D}{\partial x} + \sigma b \frac{\partial D}{\partial x}$$

$$= \left(\int_\sigma^0 \frac{\partial}{\partial \sigma'}(b\sigma') d\sigma' + \sigma b \right) \frac{\partial D}{\partial x}$$

$$= 0. \qquad (19)$$

Thus, the across-isobath (x) component of the internal pressure gradient vanishes in this case also.

3. The discrete pressure gradient

In this section we examine the error in the finite difference pressure gradient for given buoyancy profiles. The first two subsections examine special cases that can be treated analytically, while the last subsection considers buoyancy profiles that are more representative of model (and ocean) data. The finite difference scheme analyzed below makes use of the Arakawa B grid (Arakawa and Lamb 1977) in the horizontal and a staggered grid in the vertical. The particular use of the B-scheme is irrelevant, however, since the critical factor leading to the truncation error in (14) is the vertical finite difference scheme that is used for the hydrostatic equation (11) that relates B to b. Quantities that are defined for the layers, such as b, B and $\delta\sigma$, are identified by integer values of the vertical index k. Quantities identified at the top and bottom of the ocean

TABLE 2. Pressure gradient error (cm s^{-1}). Reference state not removed.

Mode number	Vertical resolution (K)						
	5	10	15	20	25	30	35
1	10.68	2.58	1.16	0.64	0.42	0.27	0.21
2	8.75	3.63	1.67	0.93	0.60	0.40	0.28
3	12.21	4.03	1.88	1.01	0.66	0.40	0.35

and at the interfaces between the layers, such as σ, are identified by half integer values of k. Denoting the K-1 interface values of σ by $\hat{\sigma}_{k+1/2}$, $k = 1, \cdots, K$-1, the layer thicknesses are defined by

$$\delta\sigma_k = \hat{\sigma}_{k-1/2} - \hat{\sigma}_{k+1/2}, \qquad (20)$$

where by definition $\hat{\sigma}_{1/2} = 0$ and $\hat{\sigma}_{K+1/2} = -1$. The caret is used to identify variables defined at the layer interfaces. From (20), it follows that

$$\sum_{k=1}^{K} \delta\sigma_k = 1. \qquad (21)$$

The layer values of σ are defined by

$$\sigma_k = \frac{1}{2}(\hat{\sigma}_{k+1/2} + \hat{\sigma}_{k-1/2}), \qquad (22)$$

from which it follows that

$$\sum_{k=1}^{K} \sigma_k \delta\sigma_k = -\frac{1}{2}. \qquad (23)$$

The finite difference approximation to (14), after multiplying by the grid size δx, is denoted PX and given by

$$PX = P1_k - \sum_{k'=1}^{K} P1_{k'}\delta\sigma_{k'} \qquad (24)$$

$$P1_k = -[\delta_x(\overline{DB}^y) + \sigma_k\overline{\bar{b}^x\delta_x D}^y]. \qquad (25)$$

In (25), standard notation for horizontal averaging and differencing is used.

Arakawa and Suarez (1983) show that the most accurate form of the hydrostatic equation is achieved by defining both buoyancy b and its integral B at the k-layers. Given K values of b_k, the integral form (10) is

$$B_k = \sum_{k'=1}^{k-1} b_{k'}\delta\sigma_{k'} + \frac{1}{2}b_k\delta\sigma_k. \qquad (26)$$

The differential form (11), defined at the interfaces between layers, is obtained by writing (26) for layer k and $k + 1$, respectively, and subtracting them. The result is

$$B_1 = \frac{1}{2}b_1\delta\sigma_1 \qquad (27a)$$

$$B_k - B_{k+1} = -\hat{b}_{k+1/2}(\sigma_k - \sigma_{k+1}), \qquad (27b)$$

where

$$\hat{b}_{k+1/2} = \frac{1}{2}(b_k\delta\sigma_k + b_{k+1}\delta\sigma_{k+1})/(\sigma_k - \sigma_{k+1}). \qquad (28)$$

Equation (28) is the finite difference analog of the mean value of b between the layers k and $k + 1$. With $\hat{b}_{k+1/2}$ defined by (28), (27) is the most accurate possible discretization of (11). When a weighted average in the form of (28) is also used to define interface values of the temperature in the vertical advection terms in

the thermodynamic equation [instead of the usual unweighted average $\hat{T}_{k+1/2} = \frac{1}{2}(T_k + T_{k+1})$], the domain integral of T^2 is no longer conserved under adiabatic processes by the finite difference scheme. However, the finite-difference analog of the energy conversion term has the same form in the kinetic energy and thermodynamic equations. If one were to use (27) and (28) for the hydrostatic equation and use the usual unweighted average for $\hat{T}_{k+1/2}$ in the thermodynamic equation, the resulting finite difference scheme would conserve the domain integral of T^2 under adiabatic processes, but it would not maintain the potential to kinetic energy conversion. These various finite-difference options and their consequences are thoroughly discussed by Arakawa and Suarez (1983) who argue for giving up conservation of T^2 in favor of maintaining the proper energy conversions and an accurate hydrostatic equation.

a. Vertically isopycnal disturbance

To examine the finite-difference pressure gradient, suppose b is independent of the vertical index k. In this case (26) along with (20) and (22) show that $B_k = -b\sigma_k$. Using this and (23), along with a finite-difference identity of the form

$$\delta_x(FG) = \bar{F}^x\delta_x G + \bar{G}^x\delta_x F \qquad (29)$$

in (25) allows (24) to be expressed as

$$PX = \overline{(\delta_x(Db) - \bar{b}^x\delta_x D}^y)\sigma_k$$

$$- \overline{(\delta_x(Db) - \bar{b}^x\delta_x D}^y) \sum_{k'=1}^{K} \sigma_{k'}\delta\sigma_{k'}$$

$$= \left(\sigma_k + \frac{1}{2}\right)\overline{\bar{D}^x\delta_x b}^y. \qquad (30)$$

Since (30) is a finite-difference analog of (16), the numerical form of the pressure gradient is exact for a vertically isopycnal disturbance.

b. Horizontally isopycnal disturbance

To examine the discrete pressure gradient analytically, suppose b is a *linear* function of z only. Thus, let

$$b_k = b_0 + N_0^2\sigma_k D, \qquad (31)$$

where b_0 is a constant buoyancy and N_0 is a constant buoyancy frequency. Substituting (31) into (26) and using (20) and (22) gives

$$B_k = -b_0\sigma_k - N_0^2 D(\hat{\sigma}_{k-1/2}^2 + \hat{\sigma}_{k+1/2}^2)/4. \qquad (32)$$

When (31) and (32) are substituted into (25) and (24), the terms containing b_0 cancel as they do in the continuous equations. Thus, PX becomes

$$PX = P2_k - \sum_{k'=1}^{K} P2_{k'}\delta\sigma_{k'}, \qquad (33)$$

where

$$P2_k$$

$$= \overline{N_0^2(\hat{\sigma}_{k-1/2}^2 + \hat{\sigma}_{k+1/2}^2)\delta_x(DD)/4 - \sigma_k^2 N_0^2 \overline{D}^x \delta_x D}^y.$$

(34)

Making use of difference identities of the form (29) as before, yields

$$PX = \epsilon_k N_0^2 \overline{\overline{D}^x \delta_x D}^y,$$

(35)

where

$$\epsilon_k = \left[\frac{1}{2}(\hat{\sigma}_{k-1/2}^2 + \hat{\sigma}_{k+1/2}^2) - \sigma_k^2\right]$$

$$- \sum_{k'=1}^{K}\left[\frac{1}{2}(\hat{\sigma}_{k'-1/2}^2 + \hat{\sigma}_{k'+1/2}^2) - \sigma_{k'}^2\right]\delta\sigma_{k'}.$$

(36)

It can be shown that (35) and (36) also hold in the more general case in which b_0 and N_0^2 are allowed to depend on y so that b depends only on z (linearly) and the along-isobath coordinate y, as in (19). Since in general, $\epsilon_k \neq 0$, the pressure gradient does not vanish in the discrete equations as it does in the continuous equations. Thus, the finite-difference scheme produces an erroneous pressure gradient in this case. The difficulty lies in the fact that the finite-difference analog of σ^2 in (36) is the average $(\hat{\sigma}_{k-1/2}^2 + \hat{\sigma}_{k+1/2}^2)/2$ rather than the more accurate local value σ_k^2. Another expression for ϵ_k is obtained by substituting

$$\hat{\sigma}_{k-1/2} = \sigma_k - \frac{1}{2}\delta\sigma_k$$

$$\hat{\sigma}_{k+1/2} = \sigma_k + \frac{1}{2}\delta\sigma_k$$

for the $\hat{\sigma}$ s in (36). The result is

$$\epsilon_k = \left(\frac{\delta\sigma_k}{2}\right)^2 - \sum_{k'=1}^{K}\left(\frac{\delta\sigma_{k'}}{2}\right)^2 \delta\sigma_{k'}.$$

(37)

From (37) it is seen that the error factor ϵ_k is equal to the difference between $(\delta\sigma_k/2)^2$ and the vertical average of this quantity. The discrete pressure gradient will be exact ($\epsilon_k = 0$) in this case only if the σ-levels are spaced *uniformly* in the vertical. If the grid spacing is smaller near the surface and larger at depth, ϵ_k will be negative in the upper ocean and positive in the deeper ocean. According to (35) the erroneous pressure gradient will tend to produce a geostrophic flow along the isobaths with shallow water to the right in the upper layers and to the left in the lower layers. For example, in an eastern boundary coastal model, in which D decreases eastward over the continental rise and slope, the error in the pressure gradient force will tend to produce a false geostrophic current that is poleward in the upper layers and equatorward in the lower layers. Above a seamount, the error corresponds to a false high pressure in the upper part of the water column and a false low

pressure in the lower part of the water column, centered over the seamount.

The false pressure gradient in (35) can be expressed as an erroneous geostrophic current parallel to the isobaths,

$$V_\epsilon = \frac{PX}{f\delta x} = \epsilon_k \frac{\overline{N_0^2}}{f} \overline{D} \frac{\delta_x D}{\delta x}^y,$$

(38)

where f is the Coriolis parameter and δx is the zonal grid size. The error depends on the bottom depth and slope, the disturbance buoyancy frequency and the error factor ϵ_k. It may be especially large in models of coastal upwelling over the continental rise and slope. In such regions the ocean departs significantly from a (removable) reference state that depends on z only. Typical values of the relevant parameters in such a region are $N_0^2 \approx 1 \times 10^{-5}$ s^{-2}, $D \approx 2 \times 10^3$ m, and $(\delta_x D)/\delta x \approx 5 \times 10^{-2}$, which gives

$$V_\epsilon \approx 10\epsilon_k \text{ (m s}^{-1}).$$

(39)

The value of ϵ_k, and therefore V_ϵ, depends on the number and placement of the σ-levels in the vertical. To investigate this dependence, consider the following parametric expression for $\hat{\sigma}_k$,

$$\hat{\sigma}_k = -\left(\frac{k-1}{K}\right)^P,$$

(40)

where P is the parameter that determines how the K σ-levels are distributed in the vertical. Uniform vertical grid spacing is obtained with $P = 1$, while increasingly finer resolution near the surface is obtained with $P > 1$. Bryan and Cox (1967) used this form with $P = 2$.

Figure 1 shows the vertical profiles of $\delta\sigma$ and V_ϵ for three (affordable) values of K with $P = 2$. In this case it can be shown from (37) that ϵ_k, and hence V_ϵ, is a linear function of σ. As seen in Fig. 1b, the false geostrophic current at the sea surface is 5 cm s^{-1} in a 10-level model but it is only 1.2 cm s^{-1} in a 20-level model. The error is the same at the ocean bottom, only opposite in sign. As noted earlier in connection with (35), the false geostrophic flow is always directed parallel to the isobaths. Figure 2 shows a similar plot of $\delta\sigma$ and V_ϵ for three values of P with $K = 20$. As P is increased above 1, the resolution is increasingly variable in the vertical and the error becomes larger. The salient part of these results are summarized in Fig. 3, which shows the maximum values of V_ϵ as a function of K for three different values of P. The curves above zero ($V_\epsilon > 0$) show the values of V_ϵ at the sea surface while the curves below zero ($V_\epsilon < 0$) show the values at the ocean bottom. The error would appear to be intolerable in models with fewer than 10 levels, and it does not fall below 1 cm s^{-1} until $K \geqslant 30$. For many problems, a false geostrophic current of even 1 cm s^{-1} parallel to the isobaths along the continental slope would be a serious error.

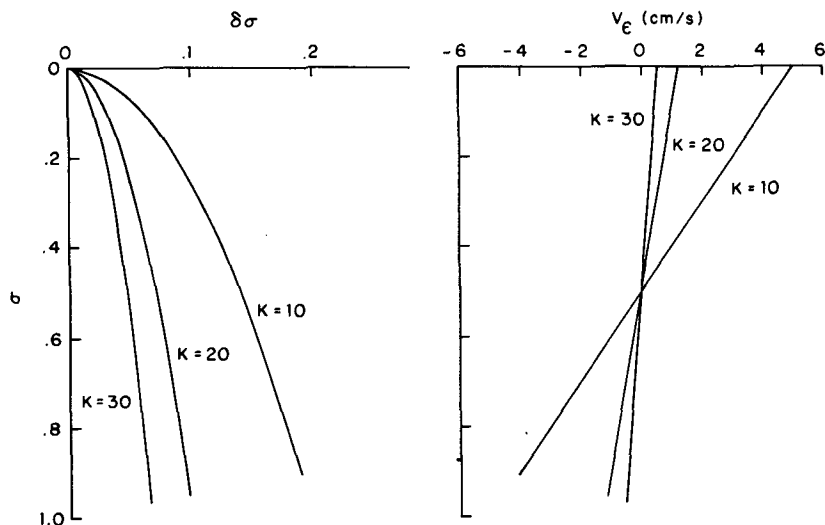FIG. 1. Profiles of (a) $\delta\sigma_k$ computed from (20) using (40) with $P = 2$ and (b) V_e computed computed from (39). Profiles are shown for $K = 10$, 20 and 30.

c. Modal buoyancy profiles

The foregoing error analysis assumes that the disturbance buoyancy is either constant with depth, or varies linearly with depth. To examine a more relevant vertical structure, the error in the discrete pressure gradient force is computed using disturbance buoyancy profiles associated with the first three baroclinic Rossby modes. The modes were computed from an analytically prescribed mean buoyancy frequency typical of the California Current region and these are shown in Fig. 4. The results presented below are not sensitive to the details of the profiles and would, therefore, be representative of any coastal region with a main thermocline having a vertical scale of several hundred meters.

The truncation error in computing the pressure gradient force from a given disturbance buoyancy profile was estimated as follows. Let $T_m(z)$ denote the temperature disturbance of unit amplitude associated with the mth vertical mode in Fig. 4, where $m = 1$, 2 or 3. If the temperature disturbance at two locations separated by a distance δx is $T_m(z)$, then, neglecting salinity effects, the resulting disturbance buoyancy $b = b_m(z)$ is the same at the two points and by (14) and (18) the internal horizontal pressure gradient vanishes. To test the discrete pressure gradient force in the presence of a sloping bottom, $T_m(z)$ was used to define a disturbance temperature profile at two grid points, separated by a distance of $\delta x = 1$ km, having an average depth of 2 km and a bottom slope of 0.05. The disturbance
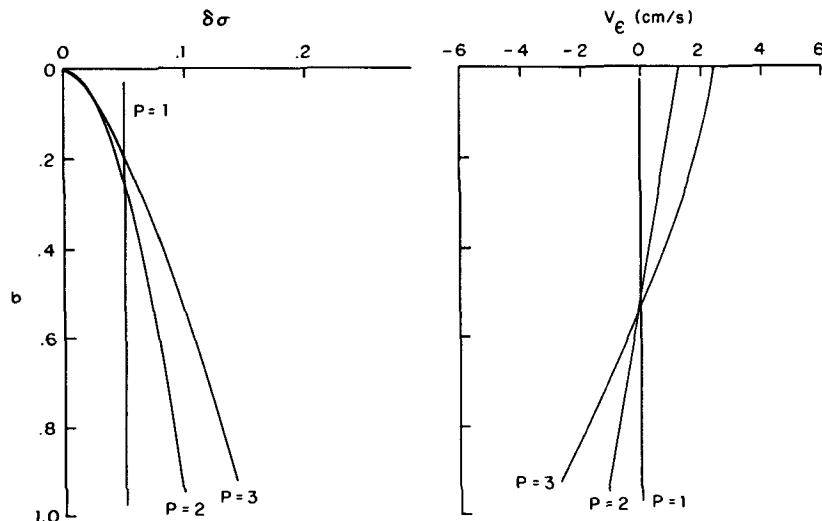

FIG. 2. Profiles of (a) $\delta\sigma_k$ computed from (20) using (40) with $K = 20$ and (b) V_e computed from (39). Profiles are shown for $P = 1$, 2 and 3.
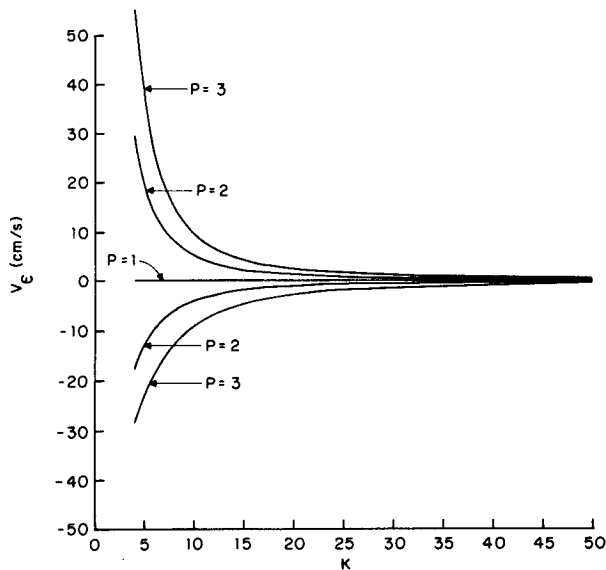
FIG. 3. Maximum values of V_e as a function of K with $P = 1, 2$, and 3. Positive values of V_e occur at the sea surface and negative values occur at the ocean bottom.

buoyancy was computed by neglecting salinity and using $b(z) = \alpha g T_m(z)$, where $\alpha = 2.5 \times 10^{-4} \, K^{-1}$ is the thermal expansion coefficient. The discrete pressure gradient force was computed from (24) using the hydrostatic equation in the form (27). Since the actual pressure gradient force is known to vanish in this case, any nonzero value computed by the finite difference scheme is the truncation error. The results are presented in Figs. 5 and 6.

The dependence of the discrete pressure gradient force error on the number and placement of the model levels in the vertical is shown in Fig. 5. For convenience, as before, the pressure gradient force errors are expressed as a geostrophic current at 38°N. The error distributions in Fig. 5 have a number of interesting features. As in the case in which $b(z)$ is linear in z (Fig. 2), the error is spread throughout the water column. A modal temperature disturbance of 1°K amplitude produces a false geostrophic current with a typical magnitude of 1–5 cm s^{-1}. The errors for all modes are distinctly larger in a 10-level model than in either a 20-level or 30-level model.

These results are summarized in Fig. 6 which shows the maximum error for each mode as a function of the number of model levels. The finite difference scheme converges since the errors approach zero as the number of vertical levels is increased. The rate of convergence is rather slow for $K > 20$, with the error in mode 3 approximately 1 cm s^{-1} for $K = 20$. Although there are many ocean modeling problems for which an erroneous geostrophic current of 1 cm^{-1} is tolerable, there are some problems for which such an error is clearly unacceptable.

The above results are based on calculations in which an optimal reference state was subtracted from the hydrostatic equation. To examine the effect that this has on the results, the calculations shown in Fig. 6 were recomputed with the reference state density $\bar{\rho}(z)$ not removed. This reference state is the same that was used to compute the modes in Fig. 4. It is based on an exponential temperature profile with an amplitude of 10°C and a scale depth of 500 m. The results, both with and without the reference state subtracted, are presented in Tables 1 and 2. The tables show the maximum truncation error in the water column for each mode as a function of the number of model levels, $K = 5, 10, \cdots 35$. By comparing the two tables it can be seen that subtracting the reference state (Table 1) reduces the truncation error only for the lower modes. The error in mode 1 is reduced by almost a factor of 3 and the error in mode 2 is reduced by about a factor of 2. However, the error in mode 3 is essentially unaffected by subtracting the reference state. These results are not inconsistent with those of Gary (1973) and Johnson and Uccellini (1983), who found that subtracting the reference state reduced the truncation error in the specific atmospheric cases that they examined. The results are also consistent with those of Sundqvist (1975) in that the truncation error associated with the higher vertical modes are largely unaffected by subtracting the reference state.

The above results can be used to estimate the pressure gradient error for any buoyancy profile that can be expressed as a linear combination of the first three modes in Fig. 4. Consider for example the density fluctuations associated with mesoscale features off the west coast of North America. Rienecker et al. (1987) showed
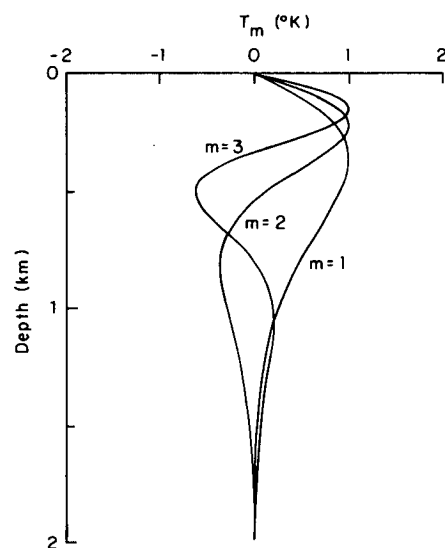

FIG. 4. The temperature disturbance of unit amplitude (1°K) associated with each of the first three baroclinic Rossby modes computed for a 2000 m deep ocean with a mean stratification representative of the California Current.
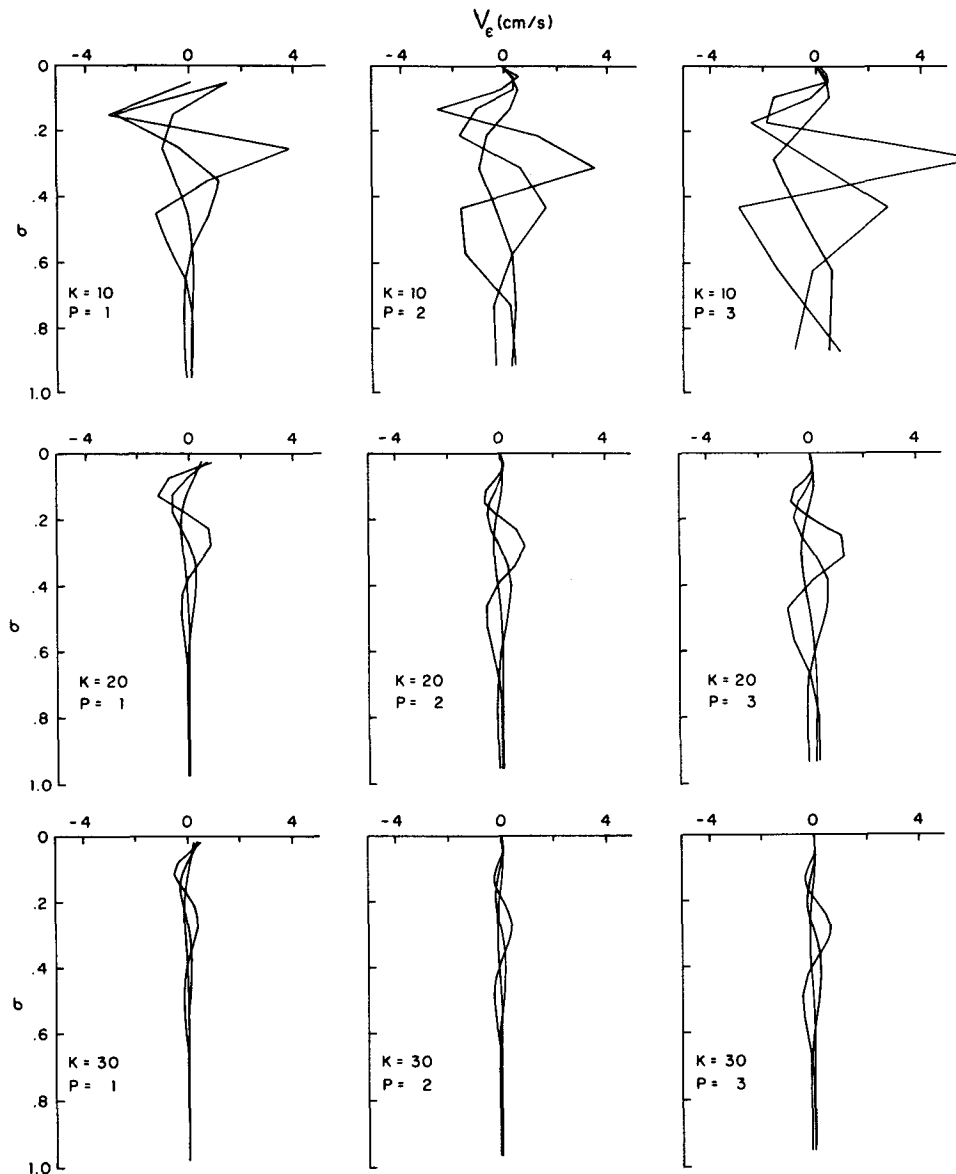
FIG. 5. Vertical profiles of the pressure gradient force error for three different values of K (top, middle and bottom row, respectively) and three different values of P (left, middle and right columns, respectively). In each frame, the errors are shown for the three disturbance temperature profiles shown in Fig. 4, and they are expressed as a geostrophic current (cm s^{-1}) at 38°N.

that over 90 percent of the variance in the water column is explained by the first EOF (empirical orthogonal function) of density. The pattern of the first EOF (Rienecker et al.'s Fig. 8a) bears a close resemblance to the third dynamical mode in Fig. 4. Considering a typical disturbance amplitude of 3°C, Tables 1 and 2 indicate that the pressure gradient error in a 10-level model over the continental rise would be about 10 or 12 cm s^{-1}, depending on whether a reference state density profile is removed or not. The corresponding error in a 30-level model would be about an order of magnitude smaller.

As a final example of the kind of error that exists near steep topography in σ-coordinate models, we show the truncation error using a horizontal and vertical resolution that results in a hydrostatically inconsistent scheme. The results shown in Fig. 6, computed with $\delta x = 1$ km, are all based on a hydrostatically consistent scheme since (1) is satisfied for $K \leqslant 50$. To examine inconsistent schemes, we recomputed the largest truncation error in the water column, as in Fig. 6, but with different values of the grid size δx. Figure 7 shows the results for $\delta x = 5$ and 10 km, respectively. With $\delta x = 5$ km (Fig. 7a), the consistency requirement (1) is sat-
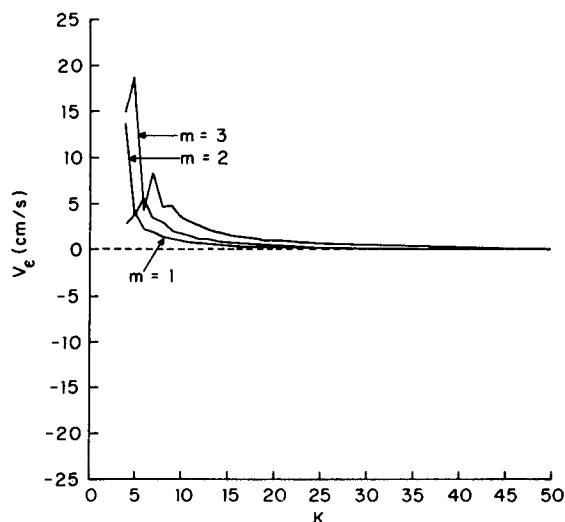
FIG. 6. Maximum value of the pressure gradient force error as a function of the number of model levels, K, for each modal temperature disturbance shown in Fig. 4. In this computation $P = 2$, however, the results are similar for $p = 1$ and 3.

isfied only for $K \leqslant 25$. Larger values of K result in sufficiently small $\delta\sigma$ that (1) is violated. In this situation the scheme does not converge, and *increasing* the vertical resolution beyond $K = 25$ results in a *larger* truncation error, as pointed out by Janjić (1977) and Mesinger (1982). As predicted by (1), the situation is worse with $\delta x = 10$ km (Fig. 7b). In this case, the scheme is hydrostatically consistent only for $K \leqslant 12$. This example clearly shows the complex nature of the pressure gradient force error in σ-coordinate models. It is obviously essential to choose the horizontal and vertical resolution carefully, not only to accommodate the particular ocean problem at hand, but also to satisfy the hydrostatic consistency condition (1).

5. Summary and conclusions

This study analyzes and documents the truncation error and the error due to hydrostatic inconsistency, associated with computing the pressure gradient force over steep topography in σ-coordinate ocean models. The intent of the study is neither to advocate nor to discredit the use of σ-coordinates for studying flow over steep topography. The purpose is simply to document the errors associated with given profiles of buoyancy and pressure typical of synoptic disturbances in the ocean. A major objective is to investigate how the errors depend on the model parameters, primarily resolution, and the vertical structure of the disturbance.

The results show that if the finite difference scheme satisfies the condition for hydrostatic consistency (1), the errors can be reduced to tolerable levels with sufficiently high resolution. For moderately high vertical resolution, e.g., $K \approx 20$, Fig. 6 and Table 1 show that

the maximum error in the water column, expressed as a geostrophic current, is a little less than 1 cm s^{-1} for a topographic slope of 0.05 and modal amplitudes of 1°K. The error is smaller for modes 1 and 2 if a proper reference state is removed. Since this analysis is linear in the slope and modal amplitude, the result can be used to estimate the truncation error associated with any other topographic slope or modal amplitude. Thus for example, the truncation error associated with a mode 3 temperature disturbance of 2°K amplitude over a topographic slope of 0.10 would be four times greater than that shown in Fig. 6. The pressure gradient error associated with mesoscale features over the continental rise off the west coast of North America using a hydrostatically consistent 30-level model is estimated to be about 1 cm s^{-1}.

No attempt has been made to analyze the influence of the truncation error on the actual performance of a
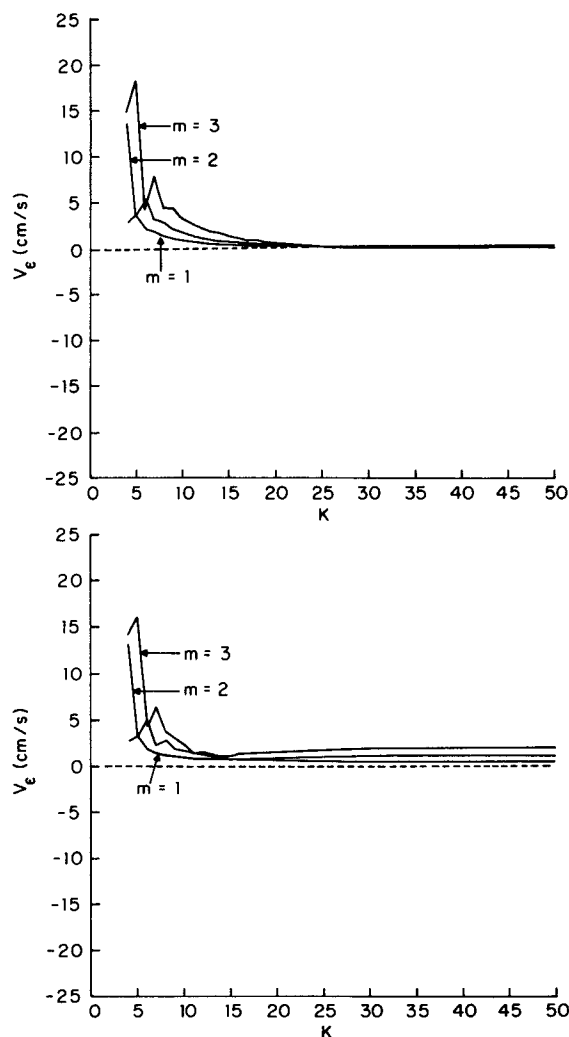

FIG. 7. As in Fig. 6 except computed with (a) δx = 5 km and (b) δx = 10 km.

model. It is important to do so however, because the truncation error is really the simplest measure of the overall accuracy of the finite difference scheme. It is likely that the effect of truncation error in a model will be much more difficult to determine than the truncation error itself. The effect is likely to depend on factors other than just the resolution. As pointed out by Arakawa and Suarez (1983), such things as the integral properties of the finite difference scheme could play a very important role in constraining the effects of the truncation errors analyzed in this study. This topic is left for a future study.

REFERENCES

Arakawa, A., and V. R. Lamb, 1977: Computational design of the basic dynamical processes of the UCLA general circulation model. *Methods in Computational Physics,* Vol 17, J. Chang, Ed., Academic Press, 173–265.

——, and M. J. Suarez, 1983: Vertical differencing of the primitive equations in sigma coordinates. *Mon. Wea. Rev.,* **111,** 34–45.

Bryan, K., and M. D. Cox, 1967: A numerical investigation of the oceanic general circulation. *Tellus,* **19,** 54–90.

Corby, G. A., A. Gilchrist and R. L. Newson, 1972: A general circulation model of the atmosphere suitable for long period integrations. *Quart. J. Roy. Meteor. Soc.,* **98,** 809–832.

CTZ Group, 1988: The coastal transition zone program. *Eos,* **69,** 698–699, 704, 707.

Gary, J. M., 1973: Estimate of truncation error in transformed coordinate, primitive equation atmospheric models. *J. Atmos. Sci.,* **30,** 223–233.

Janjić, Z. I., 1977: Pressure gradient force and advection scheme used for forecasting with steep and small scale topography. *Contrib. Atmos. Phys.,* **50,** 186–199.

Johnson, D. R., and L. W. Uccellini, 1983: A comparison of methods for computing the sigma-coordinate pressure gradient force for flow over sloped terrain in a hybrid theta-sigma model. *Mon. Wea. Rev.,* **111,** 870–886.

Mesinger, F., 1982: On the convergence and error problems of the calculation of the pressure gradient force in sigma coordinate models. *Geophys. Astrophys. Fluid Dyn.,* **19,** 105–117.

——, and Z. I. Janjić, 1985: Problems and numerical methods of the incorporation of mountains in atmospheric models. *Lect. Appl. Math.,* **22,** 81–120.

Rienecker, M. M., C. N. K. Mooers and A. R. Robinson, 1987: Dynamical interpolation and forecasts of the evolution of mesoscale features off Northern California. *J. Phys. Oceanogr.,* **17,** 1189–1213.

Rousseau, D., and H. L. Pham, 1971: Premiers resultat d'un modele de prevision numerique a courte echeance sur l'Europe. *La Meteorologie,* **20,** 1–12.

Simmons, A. J., and D. M. Burridge, 1981: An energy and angular-momentum conserving vertical finite difference scheme and hybrid vertical coordinates. *Mon. Wea. Rev.,* **109,** 758–766.

Sundqvist, H., 1975: On truncation errors in sigma-system models. *Atmosphere,* **13,** 81–95.

——, 1976: On vertical interpolation and truncation in connexion with use of sigma-system models. *Atmosphere,* **14,** 37–52.